2003-185-N0 -- HIGH-POWER BEAM DUMP FOR A LARGE ACCEPTANCE RIA FRAGMENT SEPARATOR

Principal Investigators: G. Savard, Physics
J. A. Nolen, Physics
C.-L. Jiang, Physics
A.F. Levand, Physics
V. Aseev, Physics

Funding Profile:
FY 2001 $0K
FY 2002 $0K
FY 2003 $61.3 K
FY 2004 $580K
FY 2005 $0K

Purpose: The Rare Isotope Accelerator (RIA) is the highest priority for new construction in nuclear physics in the U.S. The main components of the RIA facility are a high-power multi-beam superconducting heavy-ion accelerator, a production complex where isotopes are created via ISOL techniques, fragmentation techniques, or new approaches combining advantages of both techniques, and finally a high-efficiency post-accelerator based on the ATLAS-like linac. All three major components rely heavily on new technologies developed at Argonne. The fragment separators in the production area have been identified as R&D issues of need that are critical to ensure the success of the project. The fragment separators that will be used at RIA to collect and separate the reaction products also will have to handle the high-power primary beam and dispose of the unwanted contaminant radioactive ions. These problems will be much more serious at RIA than in any previous accelerator, and a workable solution is required for the proper operation and containment of the high-level of radioactivity to areas with proper nuclear classification.

Approach: The novel concept of stopping fragmentation products in a large gas cell before reacceleration requires a very high performance from the fragment separator feeding the ions into the gas cell. This separator must also be able to accept the very high power beam and radioactive contaminant also produced in the primary target. We have studied the key ingredients determining the resolution of fragment separators and identified and characterized the main sources of contamination. Basic requirements for a more advanced design for the fragment separation that removes these limitations have been identified and a possible ion optical solution has been laid out and studied to first order. The main locations where radioactive contaminants can be dumped have been identified and possible layouts for beam dumps capable of handling beam power and radioactivity are being studied.

Technical Progress and Results: The work performed this year can been separated along 3 lines of development that will lead us to a proper technical solution: 1) the locations where different reaction products can be produced must first be identified and the extent of the contamination characterized; 2) these reaction products and the primary beam must then be transported and the locations where they will deposit energy identified and the power deposition density estimated; and finally, 3) the technology required to meet the requirements obtained from 1) and 2) must be developed. Progress on all three fronts is described below.

The first task is the identification of the isotopes produced in the fragment separator. This task is further complicated by the fact that the fragment separators will use various primary beams and reactions to produce different reaction products and that each case will vary from the others. The approach selected in this case is to develop the basic tools required to simulate the production and to run a number of representative cases that will outline the problem.

A new computer code was developed to perform these calculations. The present version of the code performs the following tasks:

- calculates production of radioactive ions in the primary target using the latest EPAX parametrization
- determines the momentum range over which these isotopes will exit this target
- finds optimum settings for the momentum selection slits in the initial section of the fragment separator
- removes the radioactive contaminants that will not meet this selection
- calculates the production of secondary recoils in the wedge by the initial reaction products
- determines the momentum to position along the wedge correlation for these fragments, including effects of non-uniformity in the wedge
- transport all of these fragments to the end of this section of the fragment separator
- provides a distribution of these fragments along the focal plane and the transmission for a given slit size

To our knowledge, no code before had allowed the effect of secondary reactions in the fragment separator wedge to be studied in any detail and the results reveal important effects that will have to be considered with beam powers of the magnitude of those available at RIA. The code has now been run for two representative cases, one using fragmentation and one using in-flight fission, to produce the isotopes of interest. We can see in Figures 1, 2 and 3 the distribution of activities traveling along the fragment separator.

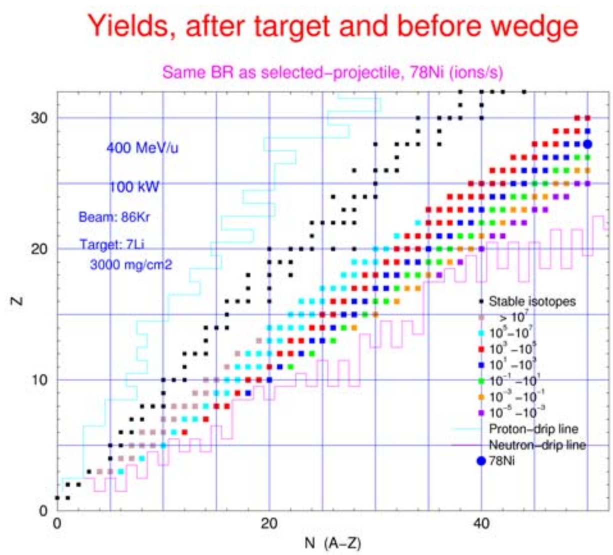

Fig. 1. Isotope distribution produced by 100kW of ^{86}Kr beam in the primary liquid lithium target.

In Figure 1, we observe the distribution of radioactive isotopes, with magnetic rigidity, Bρ, similar to the isotope of interest, produced in the primary 3 g/cm^2 flowing liquid lithium target by a 100 kW beam of ^{86}Kr at 400 MeV/u. The experiment is aimed at producing isotopes of ^{78}Ni which are highlighted by the blue circle. The intensity and the wealth of other isotopes also produced in this reaction are also shown, color coded according to intensity. Such a high rate of activity is intolerable for most experiment and the role of the fragment separator is to clean up this picture.

Figure 2 shows the yield of the various isotopes after the wedge in the fragment separator. These isotopes are either isotopes produced in the primary target that have survived the momentum cut and the wedge degrader, or isotopes produced in the wedge degrader by those primary isotopes.

It is clear that the fragmentation of the radioactive beams in the wedge generates numerous other species in quantities similar to the original production. This is because at these energies, the wedge is thick enough to yield a high nuclear reaction probability. This isotope distribution is then transported and selected by slits at the achromatic focal point at the end of this section. The isotope distribution making it past this selection is shown in Figure 3.

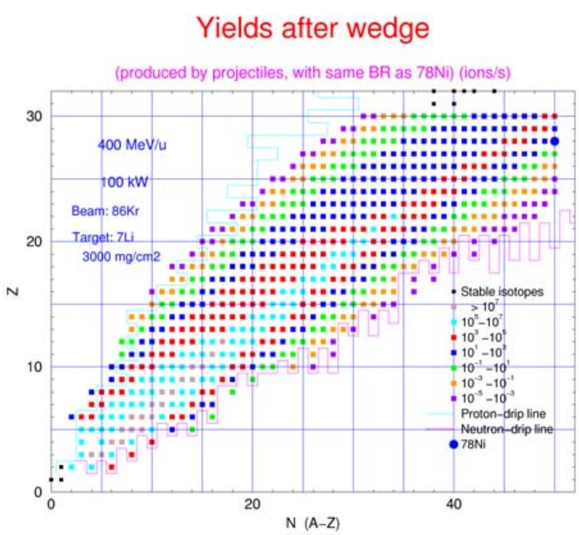

Fig. 2. Isotope distribution present after the wedge and coming either from primary production or secondary production in the wedge.

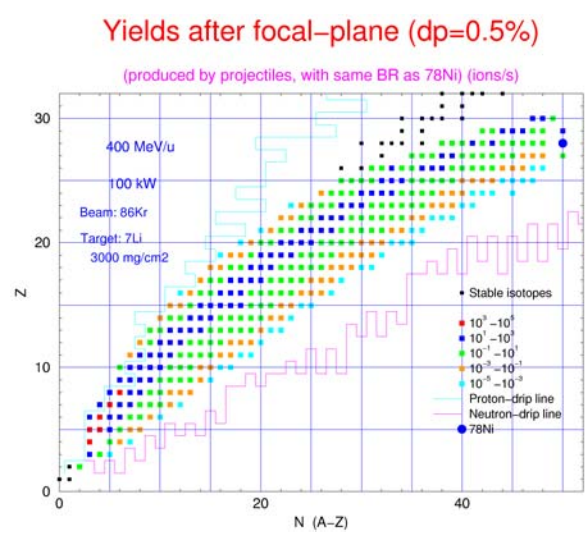

Fig. 3. Final isotope distribution after all selections for an isotope separator tuned to extract ^{78}Ni isotopes (blue circle).

Figure 3 is a realistic look at what will come together with the selected isotope (^{78}Ni in this case) with powerful beams such as those that RIA can deliver, and that is a very sobering picture. The primary beam intensity hitting the target corresponds to 1.8 X 10^{13} ^{86}Kr ions per second. The reaction products that reach the wedge degrader, that is to say that they have similar magnetic rigidity as the isotopes of interest and cannot be removed without also removing isotopes of interest, total 2.9 X10^9/s. A similar number is observed after the wedge but over a much broader range of species due to fragmentation reaction in the wedge. After the final slits we still observe about 1.6 X 10^5 radioactive ions per second, among those 10 ions per second of ^{78}Ni, the isotope of interest. We however observe that the vast majority of the contaminants that are left are radioactive ions generated by reactions in the wedge that were not present in Figure 1. This dramatic effect is the dominant source of background and was not present in previous calculations where reactions in the wedge were not included. The code also indicates the size of the final slit required to not loose too large a fraction of the isotopes of interest and the Bρ of the other isotopes created in the initial target. This is particularly important since the total power in these secondary isotopes can be tens of kilowatts, much more than the primary beam in existing facilities, and must be handled properly.

These first results with the new code are most interesting in that they yield the required Bρ distribution of the power that must be absorbed. They also yield the activity distribution that must be contained. Refinements to this code are still needed and more cases must be run but clearly this is a great progress and much insight in the separator design has already been gained by this effort in particular with respect to the use of a pre-separator that will remove most ions that might otherwise reach the final wedge degrader.

A more general picture of the source of contamination can be obtained by varying parameters such as the wedged degrader thickness for example as is shown in Figure 4. We see a clear increase in the background for thicker degraders related to production in the wedge. Similar graphs have been obtained for in-flight fission.

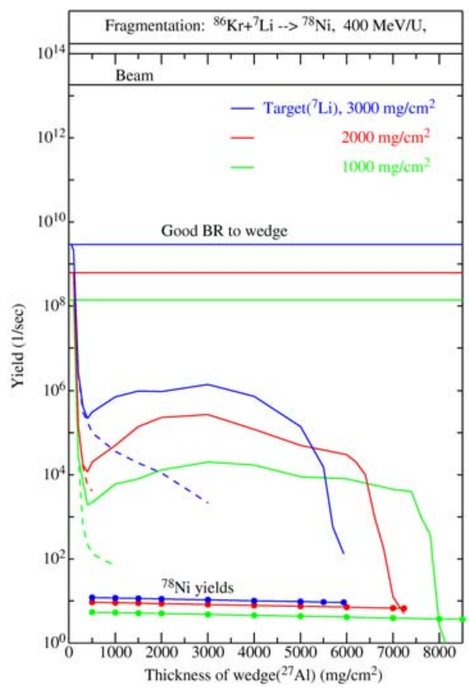

Fig. 4. Variation of the yield of ^{78}Ni and of the total contamination after the final slits as a function of the wedged degrader thickness. The top line is the beam intensity, the horizontal blue, red and green lines are the amount of contamination reaching the wedge for various target thicknesses, the curved lines are the contamination yield after the final slits and the bottom lines are the yield of ^{78}Ni after the final slits.

The next step in our approach consists of devising an actual ion package with proper output to visualize the trajectories followed by the primary beam and radioactive fragment beams whose Bρ distribution is determined in step 1. This is done within the framework of GIOS that we are modifying to improve its outputs and add the optical elements required in a fragment separator. A study of the x and y envelopes of secondary beams obtained with this improved simulation of the layout initially proposed in the Grunder committee report for one of the fragment separators at RIA confirms the finding of groups at GSI and RIKEN that such a separator cannot perform the task of cleaning up the reaction products at RIA. The next step is therefore to develop layouts more suitable to this task including a pre-separator section that will remove most of the activity before it reaches the final wedge. Such layouts have been generated for both the high-energy separator and the separator leading to the gas catcher system. We have now started feeding the information obtained in step 1 and determining typical energy deposition distribution in this separator. Results obtained with this large acceptance separator (± 9% momentum acceptance, ± 50 mrad angular acceptance in both x and y directions) are yielding interesting information with respect to the beam dump location. Because of the large momentum acceptance, it is found that the primary beam (shown as circles of different colors depending on the energy separation from the reaction products in Figure 5) is not separated from the reaction products in the first dipole magnet (left of Figure 5) but can be separated in the following quads (right of Figure 5).

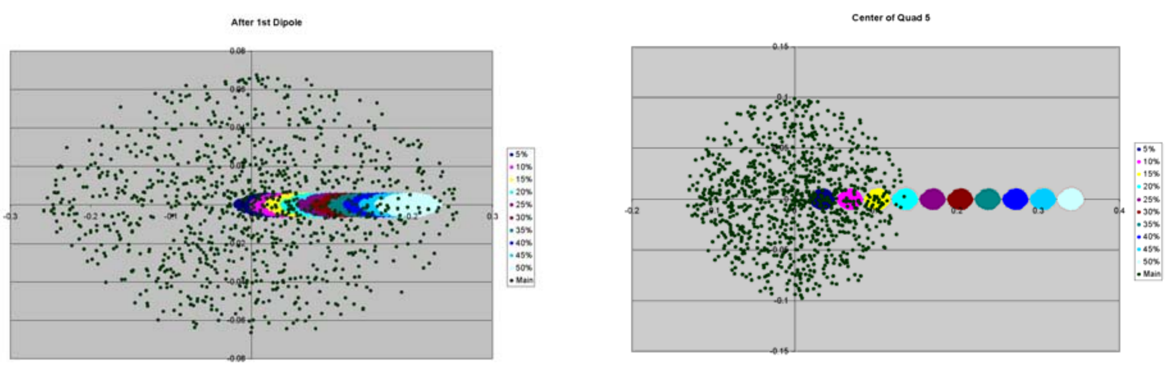

Fig. 5. X AND Y distribution of reaction product acceptance in green, size and position of primary beam for different energy difference varying from 0% to 50%. The left panel represents the distribution inside the first dipole, the right panel is in the following quadrupoles.

A beam stop could be located around the quadrupole location. The primary beam still carries typically about half of the initial beam power. The beam properties of the primary beam are still good after going through the primary target and the beam size at the dump is calculated to be typically about 3 centimeters diameter. This corresponds to an energy deposition of about 5 kW/cm^2 when this beam hits a surface with normal incidence. This power deposition is above what essentially all solid materials can tolerate. Since this power density can occur essentially at all locations on both sides of the reaction products (depending on the relative $B\rho$ of the reaction products and beam), an approach compatible with a movable beam dump is required. The basic design envisioned involves maximizing the surface area over which the beam impinges by tilting the beam dump in one or both planes. This reduces the power density but the total power is still high and must still be removed. Essentially 50 kW of cooling power must be available on each side of the magnet, most probably from cooling water, and high heat transfer must be achieved between the shield and the water. A final consideration must be to minimize secondary reactions and the generation of neutrons and that implies that the stopping must be done in high-Z material. A refractory high-Z material joined to a copper backing for high thermal conductivity might be able to handle such power load. Techniques to improve the heat transfer between the metal backing and the cooling water are being investigated as this appears to be the limiting factor in such an approach.

Auxiliary beam dumps for the high power contaminants closer to the reaction products of interest must still be considered. More calculations will be required to define the requirements here but the power deposition here, although still high, will be closer to those that have been dealt with in the past.

We plan to continue the calculations started and obtain complete layouts and higher order optical designs for both separators, update our software to handle secondary production and separation in both separator and pre-separator, run different representative cases through them to obtain purity and fragment and beam distributions, use them to obtain complete requirements for the beam dump power and location variability required, and attain a workable design for the beam dump system and distribution of contamination.

Specific Accomplishments: Preliminary results on the calculations of the production of contaminants in the intermediate wedge of the fragment separators have been presented at the RNB6 international conference and will appear in its proceedings in *Nuclear Physics A* under the title "The influence of Secondary Reactions at the Wedge of a Magnetic Separator at RIA", C.L. Jiang, *et al.*